Letter

Control of magnetic response in curved stripes by tailoring the cross section

Kostiantyn V. Yershov [1,2,*] and Denis D. Sheka [3,†]

[1] *Leibniz-Institut für Festkörper- und Werkstoffforschung, IFW Dresden, 01171 Dresden, Germany*

[2] *Bogolyubov Institute for Theoretical Physics of the National Academy of Sciences of Ukraine, 03143 Kyiv, Ukraine*

[3] *Faculty of Radiophysics, Electronics and Computer Systems, Taras Shevchenko National University of Kyiv, 01601 Kyiv, Ukraine*

(Received 9 January 2023; revised 14 March 2023; accepted 15 March 2023; published 24 March 2023)

Curved magnetic architectures are key enablers of prospective magnetic devices with respect to size, functionality, and speed. By exploring geometry-governed magnetic interactions, curvilinear magnetism offers a number of intriguing effects in curved magnetic wires and curved magnetic films. The applicability of the current micromagnetic theory requires that the sample has a constant width and thickness, which does not correspond in many cases to the specificity of experimental sample preparation. Here, we put forth a self-consistent micromagnetic framework of the curvilinear magnetism of nanowires and narrow stripes with a spatially inhomogeneous cross section. The influence of the varying cross section is exploited and illustrated by an example of the simplest topological texture, which is a transversal head-to-head (tail-to-tail) domain wall. The cross-section gradient becomes a source of domain wall pinning which competes with the curvature gradient. Eigenfrequencies of the domain wall free oscillations at the pinning potential are determined by both curvature and cross-section gradients. Prospects for curvilinear magnonics and spintronics are discussed.

DOI: 10.1103/PhysRevB.107.L100415

Introduction. The manipulation of the material response of objects using its geometrical properties became an important topic of contemporary physics. In the case of magnetism a mutual interplay of magnetization texture (material properties), curvature, and topology (geometrical properties) becomes a playground for curvilinear magnetism [1]. This rapidly developing research area of modern magnetism is aimed to explore geometry-induced effects in curved magnetic wires and films. The active exploration of this new material class shines a light on the fundamentals of the magnetism of nano-objects with curved geometry and applications of three-dimensional (3D)-shaped curved magnetic nanoarchitectures, leading to remarkable developments in shapable magnetoelectronics, magnetic sensorics, spintronics, 3D magnonics, and microrobotics [2].

An existing micromagnetic framework of curvilinear magnetism requires that samples possess an inalterable cross section with constant width and thickness [2–4]. In real experiments the width and thickness of samples can vary in a wide range. In particular, the thickness gradients of 2D film are often achieved using moving shutters [5], and plasma-enhanced chemical vapor deposition methods [6]. In nanosphere lithography there appears a thickness gradient across the cap structure with the thickest film at the top of the cap and the thinnest film close to the equator due to the specificity of the sample preparation using magnetron sputtering [7,8]. The specially varying width of the planar stripes in the form of notches and protrusions can pin or even boost domain walls [9–12]; in asymmetric nanorings changes in the stripe width become the geometrical sources of domain wall nucleation [13] and its automotion [14]. Highly spatially varying thickness gradients are achieved with 3D nanopatterning using focused-electron-beam-induced deposition (FEBID). In particular, namely the thickness gradient is expected to be a dominant mechanism of experimentally observed domain wall automotion in 3D interconnectors [15]. The space modulation of the diameter in nanowires becomes the main source of the domain wall pinning [16].

Here, we present a generalized micromagnetic framework of curvilinear wires and stripes with varying cross section, e.g., with thickness and (or) width gradients. This theory allows us not only to predict the geometry-induced effects in conventional materials, but also to explain recent experiments [14,15,17] and propose applied routes to explore the utility of 3D-shaped curved magnetic architectures for curvilinear spintronics and curvilinear magnonics. We apply the theory to predict the effects in the static and linear dynamics of domain walls in curved stripes with varying cross section. In particular, the domain wall can be pinned by local cross-section deformation; the eigenfrequencies of the domain wall free oscillations at the pinning potential are determined by both curvature and cross-section gradients.

Results. We aim to construct a theory of thin curved ferromagnet wires and stripes with varying cross section. For this purpose we represent a ferromagnet body as a space domain $\boldsymbol{r} = \boldsymbol{\gamma} + \zeta_1 \boldsymbol{e}_{\mathrm{N}} + \zeta_2 \boldsymbol{e}_{\mathrm{B}}$. Here, $\boldsymbol{\gamma} = \boldsymbol{\gamma}(s)$ described the central curve with s being the arc length coordinate, ζ_1 and ζ_2 parametrize the perpendicular cross section with varying area $S = S(s)$, and unit vectors $\boldsymbol{e}_{\mathrm{N}}$ and $\boldsymbol{e}_{\mathrm{B}}$ determine the normal and binormal direction to the central curve, respectively. Let us focus on a classical biaxial ferromagnet with the simplest energy density, $W = W^{\mathrm{X}} + W^{\mathrm{A}}$. Here, $W^{\mathrm{X}} = -A\boldsymbol{m} \cdot \nabla^2 \boldsymbol{m}$ is

*k.yershov@ifw-dresden.de

†sheka@knu.ua

the exchange energy density with A being the exchange constant, $\boldsymbol{m} = \boldsymbol{M}/M_s$ being the normalized magnetization, and M_s being the saturation magnetization. The next term, $W^{\mathrm{A}} = -K_{\mathrm{T}}^{\mathrm{eff}}(\boldsymbol{m}\cdot\boldsymbol{e}_{\mathrm{T}})^2 + K_{\mathrm{B}}^{\mathrm{eff}}(\boldsymbol{m}\cdot\boldsymbol{e}_{\mathrm{B}})^2$, describes the density of biaxial anisotropy energy with $K_{\mathrm{T}}^{\mathrm{eff}} = K_{\mathrm{T}} + 4\pi M_s^2 k_{\mathrm{T}}^{\mathrm{ms}}$ and $K_{\mathrm{B}}^{\mathrm{eff}} = K_{\mathrm{B}} + 4\pi M_s^2 k_{\mathrm{B}}^{\mathrm{ms}}$ being the anisotropy coefficients of the tangential easy axis and binormal hard axis, respectively, and $K_{\mathrm{T}} > 0$ and $K_{\mathrm{B}} > 0$ being magnetocrystalline anisotropy constants. Terms $k_{\mathrm{T}}^{\mathrm{ms}}$ and $k_{\mathrm{B}}^{\mathrm{ms}}$ arise from the magnetostatic contribution (see Supplemental Material Sec. SM-1 [18] for details).

The energy of the curved magnet is well known [2] to be restructured in the curvilinear reference frame, which follows the sample geometry, providing the means to recover the translation invariance of the effective anisotropy. The total energy, normalized by $E_0 = 4\pi M_s^2 \ell^3$, has the form $\mathcal{E} = E/E_0 = \int \mathscr{E}(\xi)d\xi$ with the energy density

$$\mathscr{E} = \mathscr{E}_0 + \underbrace{\mathscr{E}_{\mathrm{A}}}_{\substack{\text{effective}\\ \text{anisotropy}}} + \underbrace{\mathscr{E}_{\mathrm{D}}}_{\substack{\text{effective}\\ \text{DMI}}}. \tag{1}$$

Here, an exchange length $\ell = \sqrt{A/(4\pi M_s^2)}$ determines a length scale of the system. The applicability of the current micromagnetic framework requires that anisotropy directions do not vary along the cross section, i.e., $\boldsymbol{e}_{\mathrm{T}} = \boldsymbol{e}_{\mathrm{T}}(s)$ and $\boldsymbol{e}_{\mathrm{B}} = \boldsymbol{e}_{\mathrm{B}}(s)$. This makes it possible to suppose that the magnetization texture remains uniform along the direction normal to the sample, which typically means that the sample thickness does not exceed several times the characteristic magnetic length scale ℓ. One more restriction is that possible deformations of the sample cross section are smooth enough [14,15,17]. These limitations specify the applicability of the theory to the description of quasi-1D objects including curved wires, stripes, and ribbons.

The first energy contribution in (1), the term $\mathscr{E}_0 = \mathcal{S} m_i' m_i'$, is a "common," regular isotropic part of the exchange interaction with $\mathcal{S} = S(\xi)/\ell^2$ being a dimensionless cross section and $\xi = s/\ell$ being the dimensionless coordinate along the central curve of the sample. The Einstein summation convention is applied here and below, where the prime denotes the derivative with respect to ξ, and indices i, j, k numerate the curvilinear coordinates and curvilinear components of magnetization. The second term, an effective anisotropy, $\mathscr{E}_{\mathrm{A}} = \mathcal{K}_{ij} m_i m_j$, comprises the intrinsic magnetocrystalline anisotropy W^{A} and extrinsic curvilinear geometry-governed contributions. The effective anisotropy coefficients are $\mathcal{K}_{ij} = \mathcal{S}(\boldsymbol{\varpi}^2\delta_{ij} - \varpi_i\varpi_j - k_{\mathrm{T}}\delta_{1i}\delta_{1j} + k_{\mathrm{B}}\delta_{3i}\delta_{3j})$ with $\boldsymbol{\varpi} = \sigma\boldsymbol{e}_{\mathrm{T}} + \varkappa\boldsymbol{e}_{\mathrm{B}}$ being the Darboux vector, determined by a reduced curvature $\varkappa = \kappa\ell$ and reduced torsion $\sigma = \tau\ell$, and δ_{ij} being the Kronecker delta; the reduced anisotropy coefficients k_{T} and k_{B} are determined in Sec. SM-1 [18]. An effective geometry-governed Dzyaloshinskii-Moriya interaction (DMI) $\mathscr{E}_{\mathrm{D}} = \varepsilon_{ijk}\mathcal{D}_i m_j m_k'$ is linear with respect to the curvature and torsion with $\mathcal{D} = 2\mathcal{S}\boldsymbol{\varpi}$ being the geometry-governed exchange-driven Dzyaloshinskii vector.

Emergent geometry-induced magnetic field. Let us discuss here the behavior of systems with a strong anisotropy. This allows us to assume that the magnetic texture, modified by the geometry, will not deviate significantly from the equilibrium state given by the anisotropy. By introducing small deviations from a strictly tangential magnetization distribution, one can obtain the energy density (1) in the following form (see Sec. SM-2 [18] for details):

$$\mathscr{E} \approx \mathscr{E}_{\mathrm{T}} - \mathcal{S}\boldsymbol{F}\cdot\boldsymbol{m} + \mathcal{S}[k_{\mathrm{T}}(\vartheta^2 + \varphi^2) + k_{\mathrm{B}}\vartheta^2],$$
$$\boldsymbol{F} = 2\mathfrak{C}\left(\varkappa' + \varkappa\frac{\mathcal{S}'}{\mathcal{S}}\right)\boldsymbol{e}_{\mathrm{N}} + 2\mathfrak{C}\varkappa\sigma\,\boldsymbol{e}_{\mathrm{B}}. \tag{2}$$

Here, the first term $\mathscr{E}_{\mathrm{T}}$ is the energy density of the strictly tangential distribution, and the second term describes the interaction with the *emergent geometry-induced* magnetic field $\boldsymbol{F}$ (see Fig. 1). Parameter $\mathfrak{C} = \pm 1$ defines the direction of magnetization along the stripe. This field causes the magnetization to tilt from the tangential distribution by the angles

$$\vartheta \approx -\frac{\mathfrak{C}}{k_{\mathrm{T}} + k_{\mathrm{B}}}\varkappa\sigma, \quad \varphi \approx \frac{1}{k_{\mathrm{T}}}\left(\varkappa' + \varkappa\frac{\mathcal{S}'}{\mathcal{S}}\right). \tag{3}$$

One can see that the cross-section gradient $\mathcal{S}'$ acts as a *geometrical source* of the ground state tilting in addition to the curvature gradient [4,19,20]. While the strictly tangential magnetization distribution in curved wires/stripes with a constant cross section can be realized only in straight or flat arc-shaped wires with constant curvature, samples with a varying cross section possess another criterion: A strictly tangential distribution is possible when $\varkappa'/\varkappa = -\mathcal{S}'/\mathcal{S}$ and $\sigma = 0$ only.

Domain wall in a planar curved stripe. We illustrate the above theory by a flat narrow curved ferromagnetic stripe of a

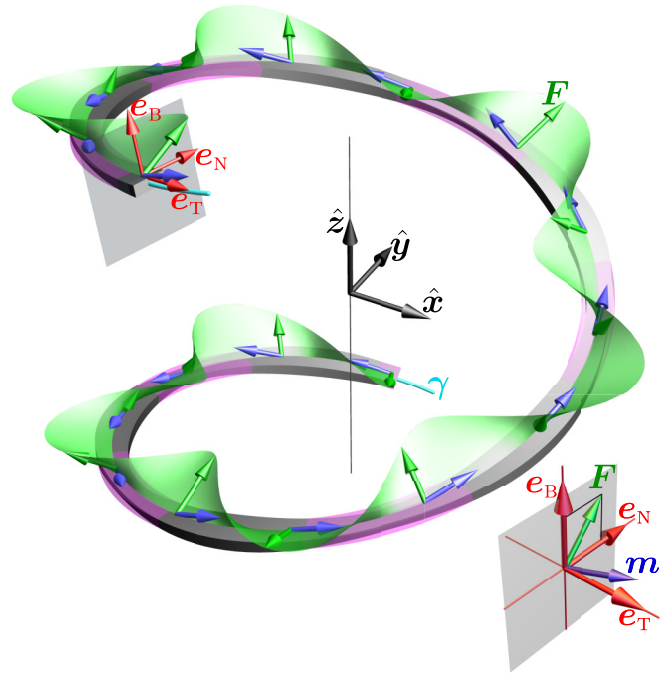

FIG. 1. Emergent geometry-induced magnetic field: Schematics of emergent field $\boldsymbol{F}$ and equilibrium magnetization texture $\boldsymbol{m}$ in a curved stripe $\boldsymbol{r}$ with spatially varying cross section. The transparent magenta color corresponds to the stripe shape without cross-section deformation. The green arrows and ribbon correspond to the direction of the field $\boldsymbol{F}$, blue arrows correspond to the equilibrium magnetization distribution, and the cyan line corresponds to the central line $\boldsymbol{\gamma}$ of the stripe.

rectangular cross section. Using a curvilinear reference frame, one can parametrize the magnetization as $\boldsymbol{m} = \boldsymbol{e}_{\mathrm{T}} \cos\theta + \boldsymbol{e}_{\mathrm{N}} \sin\theta \cos\phi + \boldsymbol{e}_{\mathrm{B}} \sin\theta \sin\phi$. The spatial-temporal evolution of magnetization follows the well-known Landau-Lifshitz-Gilbert equations, and its curvilinear form is represented in Sec. SM-3 [18].

We start with the static case, when the minimization of the energy results in a planar texture within the stripe plane with $\cos\phi = \mathcal{C} = \pm 1$ and planar deviations from the tangential direction described by $\theta(\xi)$, which satisfies the driven dissipative nonlinear pendulum equation

$$\theta'' + \frac{\mathcal{S}'}{\mathcal{S}}\theta' - k_{\mathrm{T}} \cos\theta \sin\theta = f(\xi), \;\; f(\xi) = -\mathcal{C}\left(\varkappa' + \varkappa \frac{\mathcal{S}'}{\mathcal{S}}\right). \tag{4}$$

The spatially dependent external force $f(\xi)$ results in the absence of a strictly tangential magnetization pattern. This force has two sources: gradient of the curvature and the gradient of the cross section [cf. (3)]. In addition, variable thickness causes an effective dissipative motion of the nonlinear pendulum: the term with the first derivative θ'. Note that one can avoid the appearance of effective dissipation by reducing to the parametric pendulum problem (for details, see Sec. SM-4 [18]).

Let us analyze how this force influences the nonlinear magnetization texture, the domain wall. We apply a collective variable approach based on the q-Φ model [21,22],

$$\cos\theta^{\mathrm{DW}} = -p \tanh\left[\frac{\xi - q(t)}{\Delta}\right], \quad \phi^{\mathrm{DW}} = \Phi(t). \tag{5}$$

When the force is absent, $f(\xi) = 0$, this model provides an exact solution of (4) for the straight stripe with constant cross section; it describes head-to-head or tail-to-tail domain walls with a domain wall width $\Delta = 1/\sqrt{k_{\mathrm{T}}}$ for $p = 1$ and $p = -1$, respectively.

The domain wall motion can be realized under the influence of the force $f(\xi)$. This dynamics can be described using collective variables $\{q, \Phi\}$, which determine the domain wall position and phase, respectively. The domain wall width Δ is assumed to be a slaved variable [23], i.e., $\Delta = \Delta[q(t), \Phi(t)]$. Such an approach is valid, when the force $f(\xi)$ can be considered as a small perturbation, which does not modify significantly the domain wall profile, i.e., when the curvature gradients and the cross-section gradients are weak on a scale of domain wall width. In equilibrium a narrow domain wall becomes pinned at the position q_0 and its angle Φ_0, which are determined by

$$\frac{\varkappa_0'}{\varkappa_0} + \frac{\mathcal{S}_0'}{\mathcal{S}_0} = \frac{\sqrt{k_{\mathrm{T},0}}}{\pi|\varkappa_0|}\left(\frac{k_{\mathrm{T},0}'}{k_{\mathrm{T},0}} + 2\frac{\mathcal{S}_0'}{\mathcal{S}_0}\right), \tag{6a}$$

$$\cos\Phi_0 = -p\,\mathrm{sgn}\varkappa_0, \quad \Delta_0 = 1/\sqrt{k_{\mathrm{T},0}}, \tag{6b}$$

where $\varkappa_0 \equiv \varkappa(q_0)$, $\mathcal{S}_0 \equiv \mathcal{S}(q_0)$, and $k_{\mathrm{T},0} \equiv k_{\mathrm{T}}(q_0)$ (see Sec. SM-3 [18] for details). The geometry-governed effective chiral DMI results in domain wall phase selectivity, which is defined by the signs of the topological charge p and the curvature $\varkappa$. While the domain wall in the stripe with a constant cross section is pinned at the curvature maxima, the pinning position in the general case is defined by a complex combination (6a) (see Fig. 2). In the following, for the sake of simplicity, we will consider stripes with a constant aspect ratio, i.e., stripes with constant anisotropy coefficients.

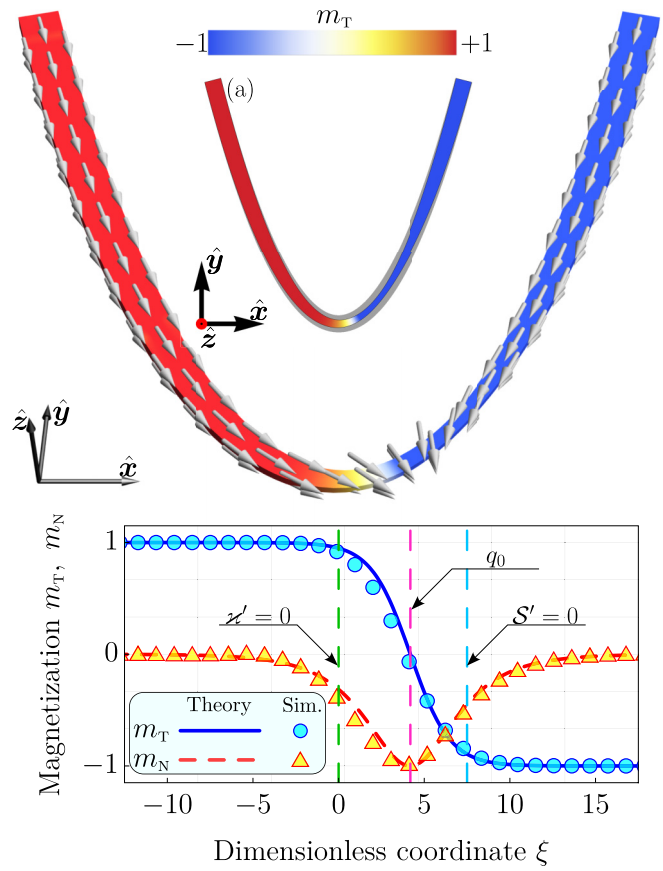

FIG. 2. Domain wall pinning: Equilibrium state of the transversal domain wall in a parabola-shaped stripe with curvature at the extremum $\varkappa_0 = 0.2$. The cross-section deformation is defined as $\mathcal{S}/\mathcal{S}_0 = 1 - \varrho/\cosh[(\xi - \eta)/\lambda]$ with $\varrho = 0.9$, $\eta = 7.5$, and $\lambda = 15$. The top inset corresponds to the magnetization distribution obtained by means of NMAG micromagnetic simulations, while the bottom inset corresponds to a comparison of simulations (symbols) and analytical predictions (solid and dashed lines). The vertical magenta dashed line is obtained with prediction (S15). Inset (a) shows the top view of the stripe geometry where the gray color corresponds to the stripe with a constant cross section.

A spatially varying curvature and cross section become sources of the domain wall dynamics. Let us consider the internal-to-system eigenmotion of the domain wall. By introducing small harmonic decaying oscillations from the equilibrium positions, we derive the domain wall eigenfrequency ω, normalized by $\omega_0 = 4\pi\gamma_0 M_s$ as $\Omega = \omega/\omega_0$,

$$\Omega \approx \sqrt{\Omega_{\mathrm{A}}\Omega_{\mathrm{g}}}, \quad \Omega_{\mathrm{g}} = \Omega_{\varkappa} + \Omega_{\mathcal{S}} + \Omega_{\varkappa\mathcal{S}},$$
$$\Omega_{\mathrm{A}} = 2\left(k_{\mathrm{B}} - \varkappa_0^2\right) + \frac{\pi}{\Delta_0}|\varkappa_0|, \quad \Omega_{\varkappa} = -\pi\Delta_0\varkappa_0'' \,\mathrm{sgn}\varkappa_0,$$
$$\Omega_{\mathcal{S}} = 2\frac{\mathcal{S}_0''}{\mathcal{S}_0}, \quad \Omega_{\varkappa\mathcal{S}} = -\pi\Delta_0\frac{\mathrm{sgn}\varkappa_0}{\mathcal{S}_0}(2\varkappa_0'\mathcal{S}_0' + \varkappa_0\mathcal{S}_0''), \tag{7}$$

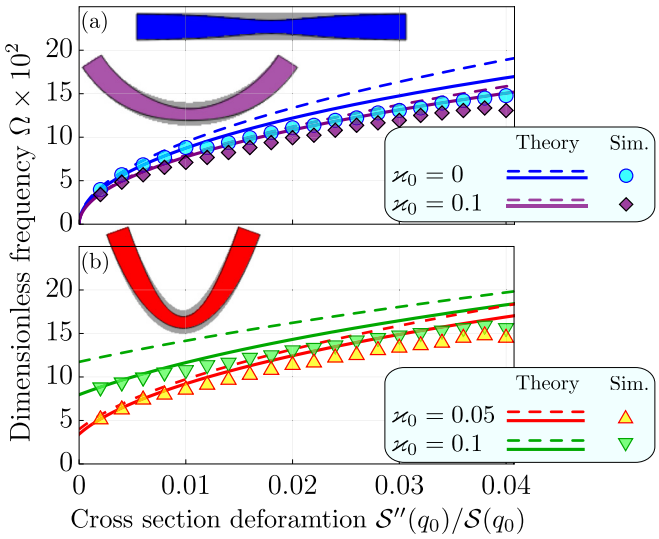

FIG. 3. Domain wall eigenoscillations. Frequencies for different geometries: (a) for rectilinear- ($\varkappa_0 = 0$) and circular-segment- ($\varkappa_0 = 0.1$) shaped stripes; (b) for parabola-shaped stripes with different curvatures at the extremum. Dashed lines correspond to the predictions (7) and solid lines correspond to prediction (S22). Symbols show the results of micromagnetic simulations (for details, see Sec. SM-5 [18]).

where γ_0 is the gyromagnetic ratio (see Sec. SM-3 [18] for details). One can see that the expression for Ω_{A} essentially depends on anisotropy constants. The next terms, $\Omega_{\varkappa}$, $\Omega_{\mathcal{S}}$, and $\Omega_{\varkappa\mathcal{S}}$, describe the influence of the curvature deformation, cross-section deformation, and their coupling onto the eigenfrequency, respectively.

In order to verify our analytical results we performed full-scale micromagnetic simulations of magnetically soft stripes within the NMAG code [24]. Permalloy is chosen as a material with the following material parameters: exchange constant $A = 26$ pJ/m, saturation magnetization $M_s = 860$ kA/m, and damping coefficient $\alpha = 0.01$. These parameters result in the exchange length $\ell \approx 5.7$ nm and $\omega_0 \approx 30.3$ GHz. In simulations the thermal effects and anisotropy are neglected. In all simulations we considered stripes with total length $L = 500$ nm and cross section defined as $\mathcal{S}(\xi) = \mathcal{s}_0\{1 - \varrho/\cosh[(\xi - \eta)/\lambda]\}$. The parameter $\mathcal{s}_0 = 75/\ell^2$ corresponds to the cross-section area on the edges with dimensions 15×5 nm^2. For detailed information, see Sec. SM-5 [18]. The results of micromagnetic simulations are in good agreement with analytical calculations (see Figs. 2 and 3).

Discussion. To study the function of varying cross section we deliberately separated the effects of curvature and torsion from those caused by the cross section. Another instructive approach is to reduce the problem of a curved magnet with varying cross section to that of a curved stripe with a fixed cross section, but with curvature, torsion, and local anisotropy modified by the varying cross section (for details, see Sec. SM-4 [18]). In this case the presented system can be treated as a chiral biaxial ferromagnet.

The developed theory of curved wires and stripes allows us to generalize existing theories [2,4] and to predict the effects in the statics and dynamics of magnetization textures depending on the deformation of the sample cross section. A spatially varying sample cross section $\mathcal{S} = \mathcal{S}(\xi)$ becomes an additional source of geometry-governed DMI and anisotropy in curved wires and stripes. Even in the simplest cases of rings ($\varkappa' = 0$, $\sigma = 0$) and helices ($\varkappa' = 0$, $\sigma' = 0$), the spatial deformation of the cross section produces a coordinate-dependent Dzyaloshinskii parameter (see Sec. SM-3 [18]), which acts similar to the functionally graded DMI [25]. One can expect similar consequences, in particular, the concept of a domain wall diode [25].

The appearance of another geometrical source of DMI has the potential to geometrically tailor the magnetochirality. Curvilinear magnetism proposes the concept of a mesoscale DMI, which unites an intrinsic DMI, determined by the material parameters, and an extrinsic DMI, determined by the local curvatures and torsion; both DMIs influence magnetic textures acting at different length scales [26]. Here, we report on another geometrical source of DMI, determined by the varying cross section. The strength of this DMI contribution can be changed by properly choosing the deformation of the cross section. Such a method to control DMI can find different applications, in particular, in artificial magnetoelectric materials [27].

Originating from the geometrical DMI, the varying cross section of the sample shows itself in emergent geometry-induced magnetic fields (2), and causes the tilting (3) of the equilibrium texture proportional to the cross-section gradient. Due to the chiral nature of DMI it can provide a chiral response for an originally achiral system similar to the influence of the gradient of the curvature [4].

In curvilinear magnonics, spin waves are known to be bound by the curvature gradient [28] in curved wires. Similarly, we expect the appearance of the effect of localization of magnon modes by the gradient of the cross section.

In curvilinear spintronics, the motion of domain walls in a curved waveguide is essentially affected by the sample curvature and torsion. In particular, the curvature gradient becomes the source of external force, which can pin the domain wall at the curvature maxima, causing the domain wall automotion, and essentially influencing domain wall mobility under external driving (for reviews, see Refs. [2,4]). We expect a series of similar effects caused by the gradient of the cross section in 2D and 3D wires and stripes in different setups [13,14,29,30], including domain wall oscillations pinned by geometrical defects [31], current-induced spin-wave emitters based on pinned domain walls [32], and the domain wall automotion in curved stripes, recently observed in Ref. [15].

We apply our theory to the problem of domain wall statics and dynamics. First, we show the effect of domain wall pinning in a planar stripe and its eigenoscillations. One can see in Fig. 2 the domain wall can be pinned in a geometrically unexpected place, defined by the combination between the curvature gradient and cross-section gradient [see (6)]. By applying a weak external field or spin current, one can excite the oscillation of the domain wall near its equilibrium position, which is described by Eq. (7). Now we illustrate eigenoscillations of the domain wall by several examples. We consider three different geometries with varying cross section: rectilinear stripes, ring segments with constant curvature, and

parabola geometry. In the case of the rectilinear stripe, the general expression for eigenfrequency (7) is reduced to $\Omega_r = 2\sqrt{k_B \mathcal{S}_0''/\mathcal{S}_0}$ and is caused by the cross-section deformation $\Omega_{\mathcal{S}}$ [see Fig. 3(a)]. In the limited case of a curved wire with a constant and circular cross section, the well-known result $\Omega = \pi\sqrt{-\varkappa_0\varkappa_0''}$ is reproduced [33]. The coupling between the curvature and the cross-section deformation, described by $\Omega_{\varkappa\mathcal{S}}$, stands out sharply for stripes with constant curvatures, in particular, for segments of a circle, which results in $\Omega = \sqrt{\Omega_A(2 - \pi\Delta_0|\varkappa_0|)\mathcal{S}_0''/\mathcal{S}_0}$ [see Fig. 3(b)]. In the case of small curvatures it results in $\Omega \approx \Omega_r[1 - (\pi/4)|\varkappa_0|\Delta_0(1 - k_T/k_B)]$. One can see that the curvature decreases the frequency for cases with $k_T < k_B$. The temporal evolution of such domain wall oscillations in a curved wire with varying cross section is presented in a video in the Supplemental Material [18]. Expression (7) for the frequency of free domain wall oscillations within the pinning potential is valid for the range of parameters $\varkappa_0 \sim 10^{-2}$ and $\mathcal{S}''(q_0)/\mathcal{S}(q_0) < 10^{-2}$. For the case of strong curvature ($\varkappa_0 \sim 10^{-1}$) and big cross-section deformations one should use the general result (S23) from Sec. SM-3 [18]. The good agreement between the analytical predictions and results of full scale micromagnetic simulations for magnetically soft stripes ($K_T = 0$ and $K_B = 0$) demonstrates that the approximation of the magnetostatic interaction by the effective biaxial anisotropy for thin and narrow stripes with a coordinate-dependent cross section is physically sound for a domain wall dynamics.

By analyzing the properties of eigenfrequencies (7) we can make some general remarks: (i) Easy-surface anisotropy k_B *increases* the eigenfrequency of the domain wall oscillations. (ii) Localized cross-section deformation also *increases* the eigenfrequency of the domain wall oscillations in the vicinity of equilibrium. (iii) However, the coupling between curvature and cross-section deformation *decreases* the eigenfrequencies. The corresponding conclusions are well presented in Fig. 3.

To conclude, we develop a micromagnetic framework of curved wires and stripes with varying cross section. Using this framework we proved the spatially varying cross section becomes another source of geometry-governed DMI on par with local curvature and torsion. It allows us to describe the effects of domain wall pinning and eigenoscillation. We expect that this theory will push different directions in curvilinear magnonics and spintronics. Its generalization for the case of curved films and shells would affect curvilinear skyrmionics as well. The proposed model can be extended for different ordered media, including curvilinear antiferromagnets [3,34–36]. The impact of such an approach goes well beyond the magnetism community. The proposed description of the vector field behavior can be applied to different emergent fields of studies of curvature effects. The prospective applications include the manipulation of molecule alignment in liquid crystals [37,38], topological textures in flexible ferroelectrics [39,40], and curved superconductors [3,41].

Acknowledgments. We thank Ulrike Nitzsche for technical support. We also appreciate discussions with Amalio Fernndez-Pacheco and Jeroen van den Brink. D.Sh. acknowledges the financial support by the program "Magnetism in Ukraine Initiative" (IEEE Magnetics Society and the Science and Technology Center of Ukraine, Project No. 9918). K.Y. acknowledges the financial support of the German Research Foundation (DFG) Grant No. YE 232/1-1.

[1] R. Streubel, P. Fischer, F. Kronast, V. P. Kravchuk, D. D. Sheka, Y. Gaididei, O. G. Schmidt, and D. Makarov, Magnetism in curved geometries (topical review), J. Phys. D **49**, 363001 (2016).

[2] *Curvilinear Micromagnetism: From Fundamentals to Applications*, edited by D. Makarov and D. Sheka, Topics in Applied Physics Vol. 146 (Springer, Cham, 2022).

[3] D. Makarov, O. M. Volkov, A. Kákay, O. V. Pylypovskyi, B. Budinská, and O. V. Dobrovolskiy, New dimension in magnetism and superconductivity: 3D and curvilinear nanoarchitectures, Adv. Mater. **34**, 2101758 (2022).

[4] D. D. Sheka, O. V. Pylypovskyi, O. M. Volkov, K. V. Yershov, V. P. Kravchuk, and D. Makarov, Fundamentals of curvilinear ferromagnetism: Statics and dynamics of geometrically curved wires and narrow ribbons, Small **18**, 2105219 (2022).

[5] P. Vishwakarma, M. Gupta, V. R. Reddy, D. M. Phase, and A. Gupta, Study of interfaces in Hf/Fe system using magneto-optical Kerr effect and soft x-ray absorption spectroscopy, Phys. Status Solidi RRL **14**, 2000177 (2020).

[6] M.-C. López-Santos, R. Alvarez, A. Palmero, A. Borrás, R. C. del Campo, M. Holgado, and A. R. González-Elipe, Micron-scale wedge thin films prepared by plasma enhanced chemical vapor deposition, Plasma Processes Polym. **14**, 1700043 (2017).

[7] T. C. Ulbrich, D. Makarov, G. Hu, I. L. Guhr, D. Suess, T. Schrefl, and M. Albrecht, Magnetization Reversal in a Novel Gradient Nanomaterial, Phys. Rev. Lett. **96**, 077202 (2006).

[8] T. C. Ulbrich, C. Bran, D. Makarov, O. Hellwig, J. D. Risner-Jamtgaard, D. Yaney, H. Rohrmann, V. Neu, and M. Albrecht, Effect of magnetic coupling on the magnetization reversal in arrays of magnetic nanocaps, Phys. Rev. B **81**, 054421 (2010).

[9] A. Himeno, T. Okuno, S. Kasai, T. Ono, S. Nasu, K. Mibu, and T. Shinjo, Propagation of a magnetic domain wall in magnetic wires with asymmetric notches, J. Appl. Phys. **97**, 066101 (2005).

[10] D. Petit, A.-V. Jausovec, D. Read, and R. P. Cowburn, Domain wall pinning and potential landscapes created by constrictions and protrusions in ferromagnetic nanowires, J. Appl. Phys. **103**, 114307 (2008).

[11] F. Garcia-Sanchez, A. Kákay, R. Hertel, and P. Asselin, Depinning of transverse domain walls from notches in magnetostatically coupled nanostrips, Appl. Phys. Express **4**, 033001 (2011).

[12] H. Y. Yuan and X. R. Wang, Boosting domain wall propagation by notches, Phys. Rev. B **92**, 054419 (2015).

[13] K. Richter, A. Krone, M.-A. Mawass, B. Krüger, M. Weigand, H. Stoll, G. Schütz, and M. Kläui, Localized domain wall nucleation dynamics in asymmetric ferromagnetic rings revealed

by direct time-resolved magnetic imaging, Phys. Rev. B **94**, 024435 (2016).

[14] M.-A. Mawass, K. Richter, A. Bisig, R. M. Reeve, B. Krüger, M. Weigand, H. Stoll, A. Krone, F. Kronast, G. Schütz, and M. Kläui, Switching by Domain-Wall Automotion in Asymmetric Ferromagnetic Rings, Phys. Rev. Appl. **7**, 044009 (2017).

[15] L. Skoric, C. Donnelly, A. Hierro-Rodriguez, M. A. Cascales Sandoval, S. Ruiz-Gómez, M. Foerster, M. A. Niño, R. Belkhou, C. Abert, D. Suess, and A. Fernández-Pacheco, Domain wall automotion in three-dimensional magnetic helical interconnectors, ACS Nano **16**, 8860 (2022).

[16] J. A. Fernandez-Roldan, A. D. Riz, B. Trapp, C. Thirion, M. Vazquez, J.-C. Toussaint, O. Fruchart, and D. Gusakova, Modeling magnetic-field-induced domain wall propagation in modulated-diameter cylindrical nanowires, Sci. Rep. **9**, 5130 (2019).

[17] D. Petit, H. T. Zeng, J. Sampaio, E. Lewis, L. O'Brien, A.-V. Jausovec, D. Read, R. P. Cowburn, K. J. O'Shea, S. McVitie *et al.*, Magnetic imaging of the pinning mechanism of asymmetric transverse domain walls in ferromagnetic nanowires, Appl. Phys. Lett. **97**, 233102 (2010).

[18] See Supplemental Material at http://link.aps.org/supplemental/10.1103/PhysRevB.107.L100415 for details of the analytical calculation, micromagnetic simulations, and movies, which includes Refs. [19–24,33,42–52].

[19] Y. Gaididei, V. P. Kravchuk, and D. D. Sheka, Curvature Effects in Thin Magnetic Shells, Phys. Rev. Lett. **112**, 257203 (2014).

[20] D. D. Sheka, V. P. Kravchuk, and Y. Gaididei, Curvature effects in statics and dynamics of low dimensional magnets, J. Phys. A: Math. Theor. **48**, 125202 (2015).

[21] A. P. Malozemoff and J. C. Slonzewski, *Magnetic Domain Walls in Bubble Materials* (Academic, New York, 1979).

[22] J. C. Slonczewski, Dynamics of magnetic domain walls, in *Magnetism and Magnetic Materials - 1971 Parts 1 and 2*, edited by C. D. Graham and J. J. Rhyne, AIP Conf. Proc. Vol. 5 (AIP, New York, 1972), p. 170, doi: 10.1063/1.3699416.

[23] *Spin Dynamics in Confined Magnetic Structures III*, edited by B. Hillebrands and A. Thiaville, Topics in Applied Physics Vol. 101 (Springer, Berlin, 2006).

[24] T. Fischbacher, M. Franchin, G. Bordignon, and H. Fangohr, A systematic approach to multiphysics extensions of finite-element-based micromagnetic simulations: Nmag, IEEE Trans. Magn. **43**, 2896 (2007).

[25] K. V. Yershov, V. P. Kravchuk, D. D. Sheka, J. van den Brink, and A. Saxena, Domain wall diode based on functionally graded Dzyaloshinskii–Moriya interaction, Appl. Phys. Lett. **116**, 222406 (2020).

[26] O. M. Volkov, D. D. Sheka, Y. Gaididei, V. P. Kravchuk, U. K. Rößler, J. Fassbender, and D. Makarov, Mesoscale Dzyaloshinskii-Moriya interaction: Geometrical tailoring of the magnetochirality, Sci. Rep. **8**, 866 (2018).

[27] O. Volkov, U. K. Rossler, J. Fassbender, and D. Makarov, Concept of artificial magnetoelectric materials via geometrically controlling curvilinear helimagnets, J. Phys. D **52**, 345001 (2019).

[28] Y. Gaididei, V. P. Kravchuk, F. G. Mertens, O. V. Pylypovskyi, A. Saxena, D. D. Sheka, and O. M. Volkov, Localization of magnon modes in a curved magnetic nanowire, Low Temp. Phys. **44**, 634 (2018).

[29] J.-Y. Chauleau, R. Weil, A. Thiaville, and J. Miltat, Magnetic domain walls displacement: Automotion versus spin-transfer torque, Phys. Rev. B **82**, 214414 (2010).

[30] D. E. Nikonov, S. Manipatruni, and I. A. Young, Automotion of domain walls for spintronic interconnects, J. Appl. Phys. **115**, 213902 (2014).

[31] O. Alejos, C. Torres, P. Hernández-Gómez, L. López-Díaz, L. Torres, and E. Martínez, A micromagnetic study of the oscillations of pinned domain walls in magnetic ribbons, J. Magn. Magn. Mater. **316**, e295 (2007).

[32] M. Voto, L. Lopez-Diaz, and E. Martinez, Pinned domain wall oscillator as a tuneable direct current spin wave emitter, Sci. Rep. **7**, 13559 (2017).

[33] K. V. Yershov, V. P. Kravchuk, D. D. Sheka, and Y. Gaididei, Curvature-induced domain wall pinning, Phys. Rev. B **92**, 104412 (2015).

[34] O. V. Pylypovskyi, D. Y. Kononenko, K. V. Yershov, U. K. Rößler, A. V. Tomilo, J. Fassbender, J. van den Brink, D. Makarov, and D. D. Sheka, Curvilinear one-dimensional antiferromagnets, Nano Lett. **20**, 8157 (2020).

[35] O. V. Pylypovskyi, Y. A. Borysenko, J. Fassbender, D. D. Sheka, and D. Makarov, Curvature-driven homogeneous Dzyaloshinskii–Moriya interaction and emergent weak ferromagnetism in anisotropic antiferromagnetic spin chains, Appl. Phys. Lett. **118**, 182405 (2021).

[36] K. V. Yershov, Dynamics of domain walls in curved antiferromagnetic wires, Phys. Rev. B **105**, 064407 (2022).

[37] G. Napoli and L. Vergori, Extrinsic Curvature Effects on Nematic Shells, Phys. Rev. Lett. **108**, 207803 (2012).

[38] G. Napoli, O. V. Pylypovskyi, D. D. Sheka, and L. Vergori, Nematic shells: new insights in topology- and curvature-induced effects, Soft Matter **17**, 10322 (2021).

[39] M. Owczarek, K. A. Hujsak, D. P. Ferris, A. Prokofjevs, I. Majerz, P. Szklarz, H. Zhang, A. A. Sarjeant, C. L. Stern, R. Jakubas, S. Hong, V. P. Dravid, and J. F. Stoddart, Flexible ferroelectric organic crystals, Nat. Commun. **7**, 13108 (2016).

[40] X. Jia, R. Guo, B. K. Tay, and X. Yan, Flexible ferroelectric devices: Status and applications, Adv. Funct. Mater. **32**, 2205933 (2022).

[41] V. Vitelli and A. M. Turner, Anomalous Coupling Between Topological Defects and Curvature, Phys. Rev. Lett. **93**, 215301 (2004).

[42] M. P. do Carmo, *Differential Geometry of Curves and Surfaces* (Dover, New York, 2016).

[43] W. Kuhnel, *Differential Geometry: Curves - Surfaces - Manifolds*, 2nd ed. (American Mathematical Society, Providence, RI, 2005).

[44] D. G. Porter and M. J. Donahue, Velocity of transverse domain wall motion along thin, narrow strips, J. Appl. Phys. **95**, 6729 (2004).

[45] A. Aharoni, Demagnetizing factors for rectangular ferromagnetic prisms, J. Appl. Phys. **83**, 3432 (1998).

[46] Y. Gaididei, A. Goussev, V. P. Kravchuk, O. V. Pylypovskyi, J. M. Robbins, D. Sheka, V. Slastikov, and S. Vasylkevych, Magnetization in narrow ribbons: curvature effects, J. Phys. A: Math. Theor. **50**, 385401 (2017).

[47] A. Mougin, M. Cormier, J. P. Adam, P. J. Metaxas, and J. Ferré, Domain wall mobility, stability and walker breakdown in magnetic nanowires, Europhys. Lett. **78**, 57007 (2007).

[48] K. V. Yershov, V. P. Kravchuk, D. D. Sheka, O. V. Pylypovskyi, D. Makarov, and Y. Gaididei, Geometry-induced motion of magnetic domain walls in curved nanostripes, Phys. Rev. B **98**, 060409(R) (2018).

[49] V. P. Kravchuk, Stability of magnetic nanowires against spin-polarized current, Ukr. J. Phys. **59**, 1001 (2014).

[50] V. V. Slastikov and C. Sonnenberg, Reduced models for ferromagnetic nanowires, IMA J. Appl. Math. **77**, 220 (2012).

[51] D. D. Sheka, O. V. Pylypovskyi, P. Landeros, Y. Gaididei, A. Kákay, and D. Makarov, Nonlocal chiral symmetry breaking in curvilinear magnetic shells, Commun. Phys. **3**, 128 (2020).

[52] D. D. Sheka, A perspective on curvilinear magnetism, Appl. Phys. Lett. **118**, 230502 (2021).